Immunity, Volume *34*

Supplemental Information

RUNX Transcription Factor-Mediated Association of *Cd4* and *Cd8* Enables Coordinate Gene Regulation

Amélie Collins, Susannah L. Hewitt, Julie Chaumeil, MacLean Sellars, Mariann Micsinai, Jeanne Allinne, Fabio Parisi, Elphège Nora, Dan J. Bolland, Anne E. Corcoran, Yuval Kluger, Remy Bosselut, Wilfried Ellmeier, Mark M.W. Chong, Dan R. Littman, and Jane A. Skok

Inventory

Figure S1. Schematic of DNA FISH probes used on murine chromosome 6 and supplemental data for wild-type thymocytes, related to Figure 1
Parts A to C describe details of our methodology to guide the reader through Figure 1. Part A details all probes used in the experiments and chromosomal distances between them. Part B describes the developmental stages of thymocyte differentiation and part C details our sorting protocol of these stages.
Part D shows the pericentromeric recruitment of *Cd4* and *Cd8* in WT cells to accompany the Cd4-Cd8 association in Figure 1, as described in the text and as referred to later in the manuscript when genetic manipulations are used.

Figure S2. Scheme of the *Cd8* locus with enhancers detailed and sorting strategy for $E8_I$ deficient or $E8_IE8_{II}$ double mutant thymocytes, related to Figure 2
Part A shows the position of enhancers that were deleted in the cells used in Figure 2.
Parts B and C detail the sorting strategy for these cells in Figure 2, as even though CD4 and CD8 change on the cell surface in many of the genetic manipulations used in the manuscript, these populations can still be accurately sorted using other markers.

Figure S3. Sorting strategy for *Cbfb*$^{F/F}$/*Lck-cre* thymocytes, related to Figure 3.
This details the particular sorting strategy required *Cbfb* deficient thymocytes used in Figure 2.

Figure S4. Generation of *Zbtb7b*$^{hd/hd}$ mice and sorting strategy for *Zbtb7b*$^{hd/hd}$ or ThPOK transgenic cells, related to Figure 4
Parts A to D detail the gene targeting strategy, and additionally PCR verification of *Zbtb7b*$^{hd/hd}$ mice used in Figure 4. Parts E and F describe the particular strategy employed to accurately sort genetically manipulated cells shown in Figure 4.

Figure S5. Scheme of the *Cd4* locus showing the proximal enhancer (PE) and sorting strategy for *Cd4* PE deficient thymocytes, related to Figure 5
This scheme of which enhancer is deleted and the sorting strategy for cells used in Figure 5.

Figure S6. Scheme of the *Cd4* locus showing the silencer (sil) and sorting strategy for *Cd4* PE deficient thymocytes, related to Figure 6
This scheme of which enhancer is deleted and the sorting strategy for cells used in Figure 6.

Figure S7. Sorting strategy for human lymphocytes CD8$^+$ T cells, CD4$^+$ T cells, or B cells and a model of *Cd4*-*Cd8* association during T cell development, related to Figure 7
Part A describes how human lymphocytes were sorted and Part B places our data into a proposed model during

thymocyte differentiation.

Supplementary Tables

Supplementary Tables give full experimental data of recruitment to pericentromeric heterochromatin, for one representative experiment of each genotype used.

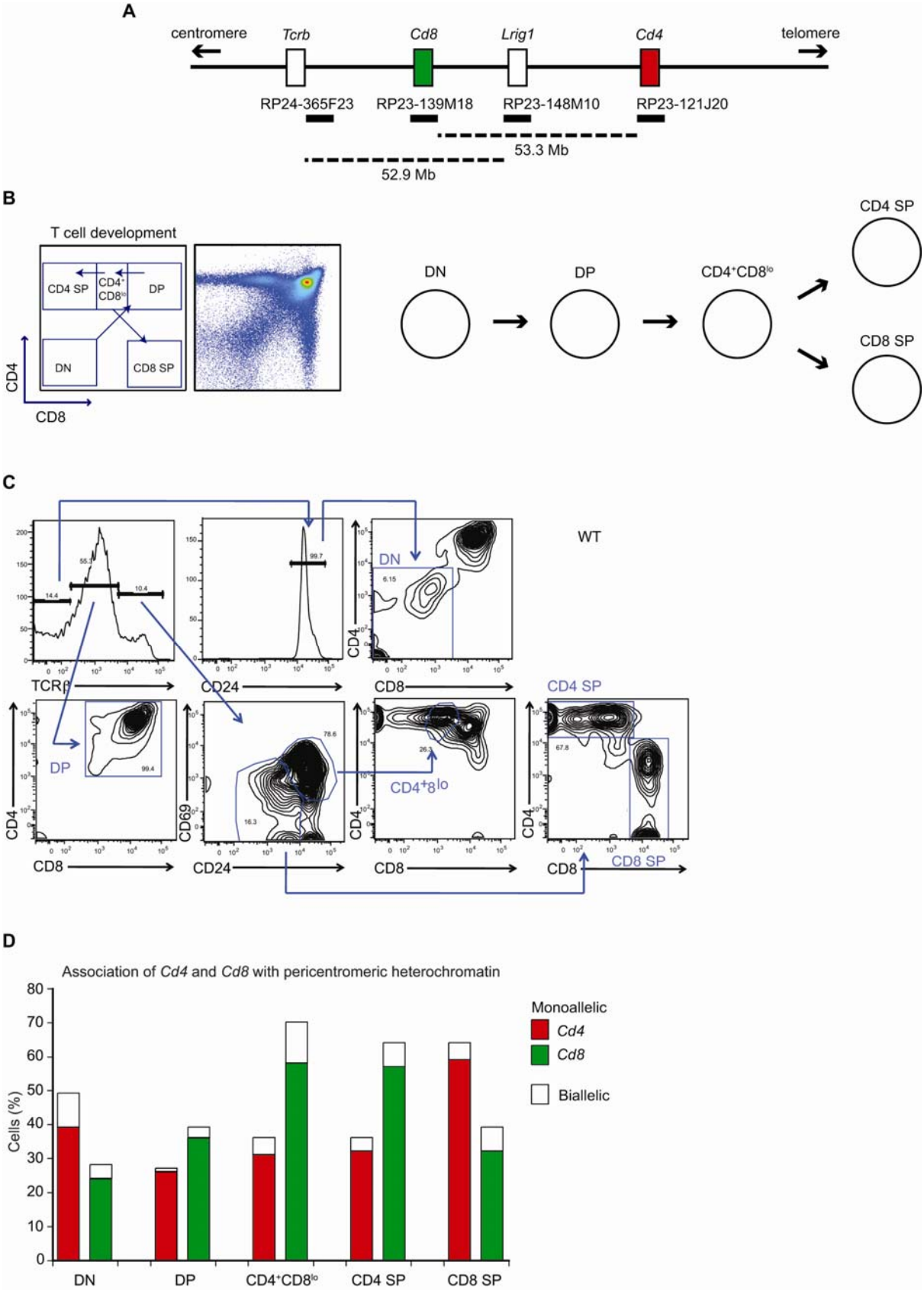

Figure S1. Schematic of DNA FISH probes used on murine chromosome 6 and supplemental data for wild-type thymocytes, related to Figure 1

(A) Location of the *Cd4* and *Cd8* loci on chromosome 6 and the BAC probes used for 3-D DNA FISH on *ex vivo* sorted cells (RP23-121J20 and RP23-139M18 for *Cd4* and *Cd8*, respectively). Also shown is the location and separation of *Tcrb* – *Lrig1* and the BAC probes used to detect these loci (RP24-365F23 and RP23-148M10, respectively).
(B) CD4 and CD8 surface expression by flow cytometry showing T cell subsets (left) and differentiation stages (right).
(C) For wild-type cells, DN were sorted as $TCRb^{lo}CD24^{+}CD4^{-}CD8^{-}$, DP as $TCRb^{int}CD4^{+}CD8^{+}$, $CD4^{+}8^{lo}$ as $TCRb^{hi}CD24^{+}CD69^{+}CD4^{+}8^{lo}$, CD4 SP as $TCRb^{hi}CD24^{-}CD69^{-}CD4^{+}$, and CD8 SP as $TCRb^{hi}CD24^{-}CD69^{-}CD8^{+}$.
(D) *Cd4* or *Cd8* recruitment to pericentromeric heterochromatin in sorted wild-type thymocytes.
3-D DNA FISH with BAC probes RP23-121J20 (*Cd4*) and RP23-139M18 (*Cd8*) was combined with a γ-satellite probe (pericentromeric heterochromatin).

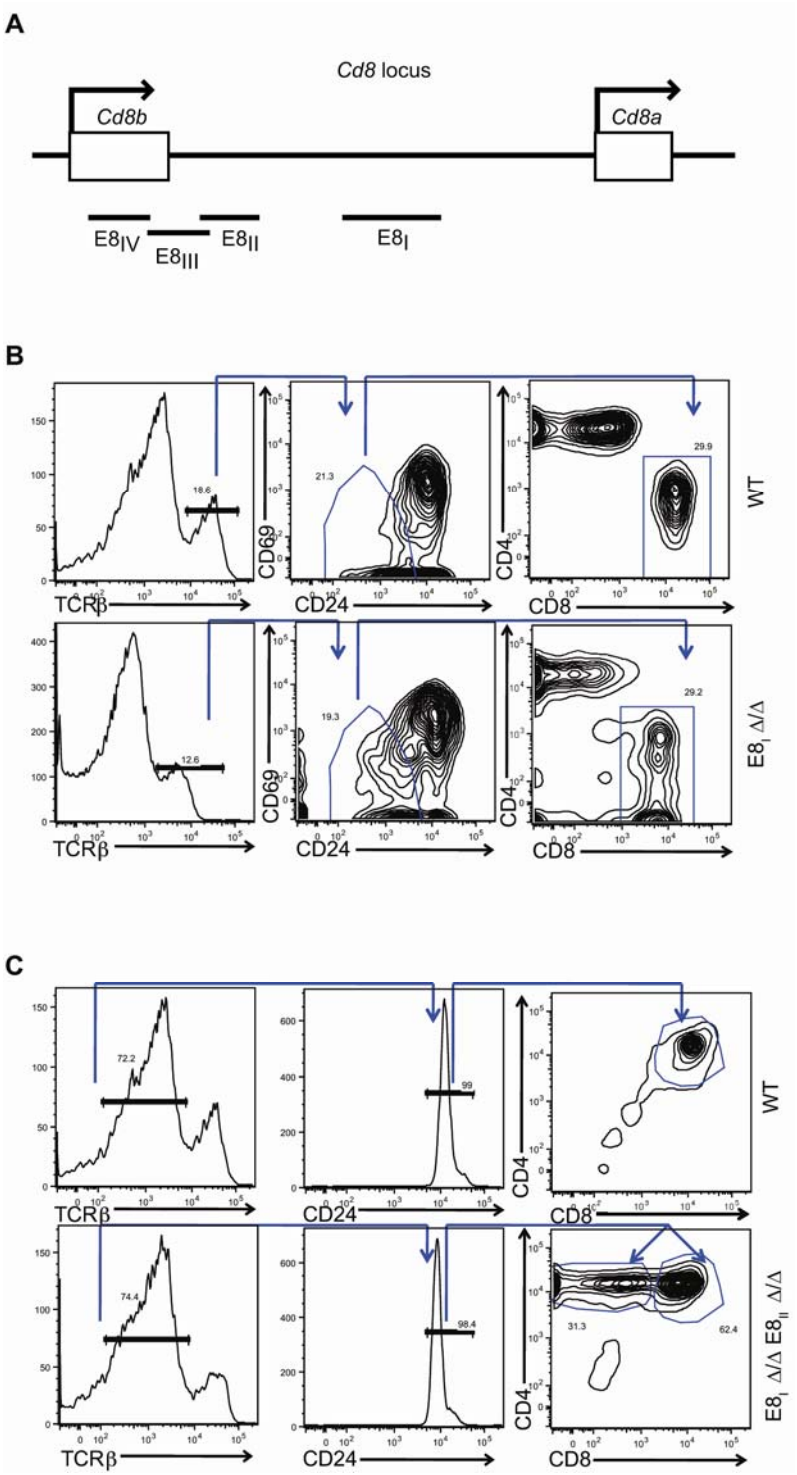

Figure S2. Scheme of the *Cd8* locus with enhancers detailed and sorting strategy for $E8_I$ deficient or $E8_IE8_{II}$ double mutant thymocytes, related to Figure 2

(A) Scheme of the *Cd8* locus with enhancers detailed.

(B) For $E8_I$ deficient cells, CD8 SP were sorted as $TCRb^{hi}CD24^{-}CD69^{-}CD8^{+}$.

(C) For $E8_IE8_{II}$ double mutant cells, $CD8^{+}$ DP were sorted as $TCRb^{int}CD24^{+}CD4^{+}CD8^{+}$, and $CD8^{-}$ DP as $TCRb^{int}CD24^{+}CD4^{+}CD8^{lo}$.

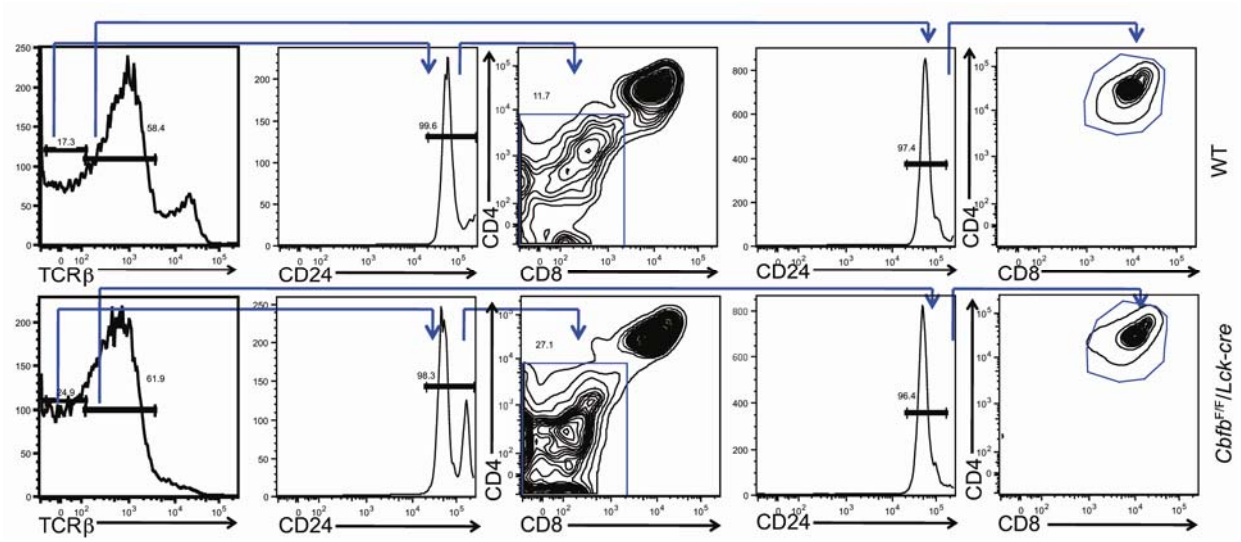

Figure S3. Sorting strategy for *Cbfb*$^{F/F}$/*Lck-cre* thymocytes, related to Figure 3.
For *Cbfb*$^{F/F}$/*Lck-cre* cells, DN were sorted as TCRb^{lo}CD24^{+}CD8^{-}, and DP as TCRb^{int}CD24^{+}CD4^{+}CD8^{+}.

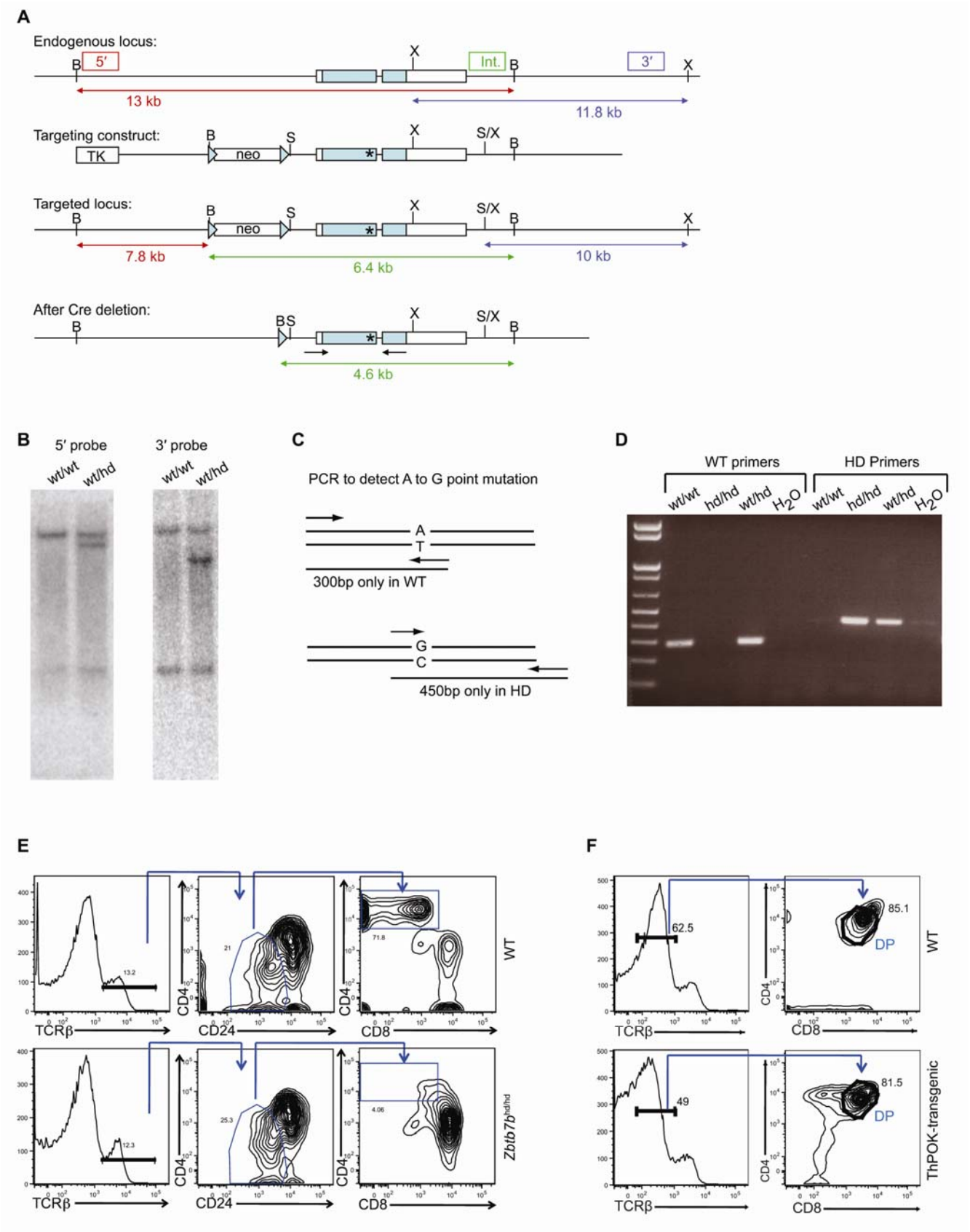

Figure S4. Generation of *Zbtb7b*$^{hd/hd}$ mice and sorting strategy for *Zbtb7b*$^{hd/hd}$ or ThPOK transgenic cells, related to Figure 4

(A) Gene targeting strategy to replace the endogenous *Zbtb7b* locus with the A to G mutation at position 389. Probe locations and fragment sizes are indicated. B, BglII; X, XbaI, S, SpeI.
(B) Southern blot analysis of untargeted (wt/wt) and targeted (wt/hd) ES cells.
(C) PCR strategy to detect the A to G point mutation in targeted mice.
(D) PCR analysis of tail DNA from *Zbtb7b*$^{wt/wt}$, *Zbtb7b*$^{hd/hd}$ and *Zbtb7b*$^{wt/hd}$ mice.
(E) For *Zbtb7b*$^{hd/hd}$ cells, CD4 SP were sorted as TCRb^{hi}CD24^{-}CD69^{-}CD4^{+}.
(F) For ThPOK transgenic mice DP cells were sorted as TCRb^{int}CD4^{+}CD8^{+}.

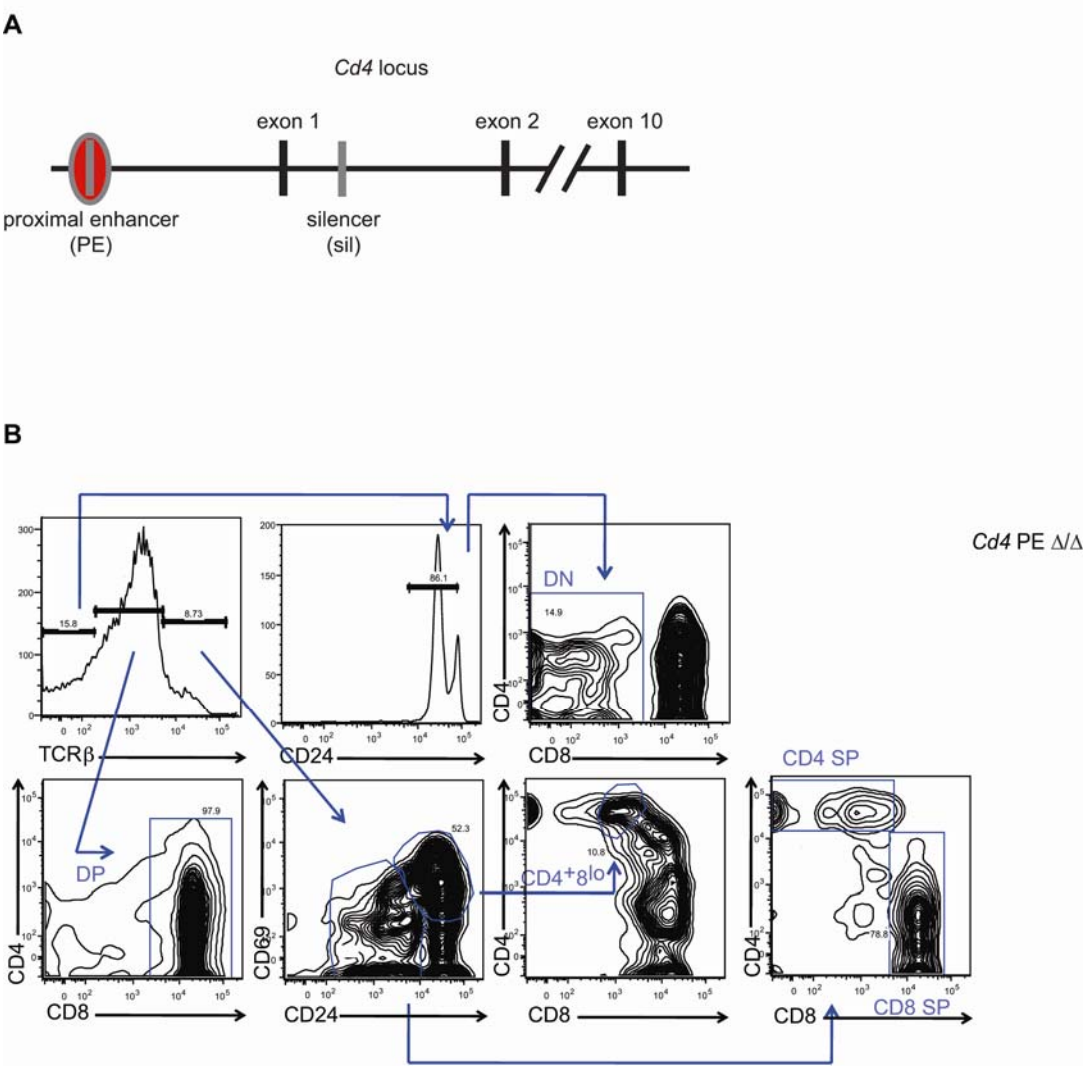

Figure S5. Scheme of the *Cd4* locus showing the proximal enhancer (PE) and sorting strategy for *Cd4* PE deficient thymocytes, related to Figure 5
(A) Scheme of the *Cd4* locus showing the position of the proximal enhancer (PE) deleted in *Cd4* PE Δ/Δ.
(B) For *Cd4* PE deficient cells, DN were sorted as TCRb^{lo}CD24^{+}CD4^{-}CD8^{-}, DP as TCRb^{int}CD8^{+}, CD4^{+}8^{lo} as TCRb^{hi}CD24^{+}CD69^{+}CD4^{+}8^{lo}, CD4 SP as TCRb^{hi}CD24^{-}CD69^{-}CD4^{+}, and CD8 SP as TCRb^{hi}CD24^{-}CD69^{-}CD8^{+}.

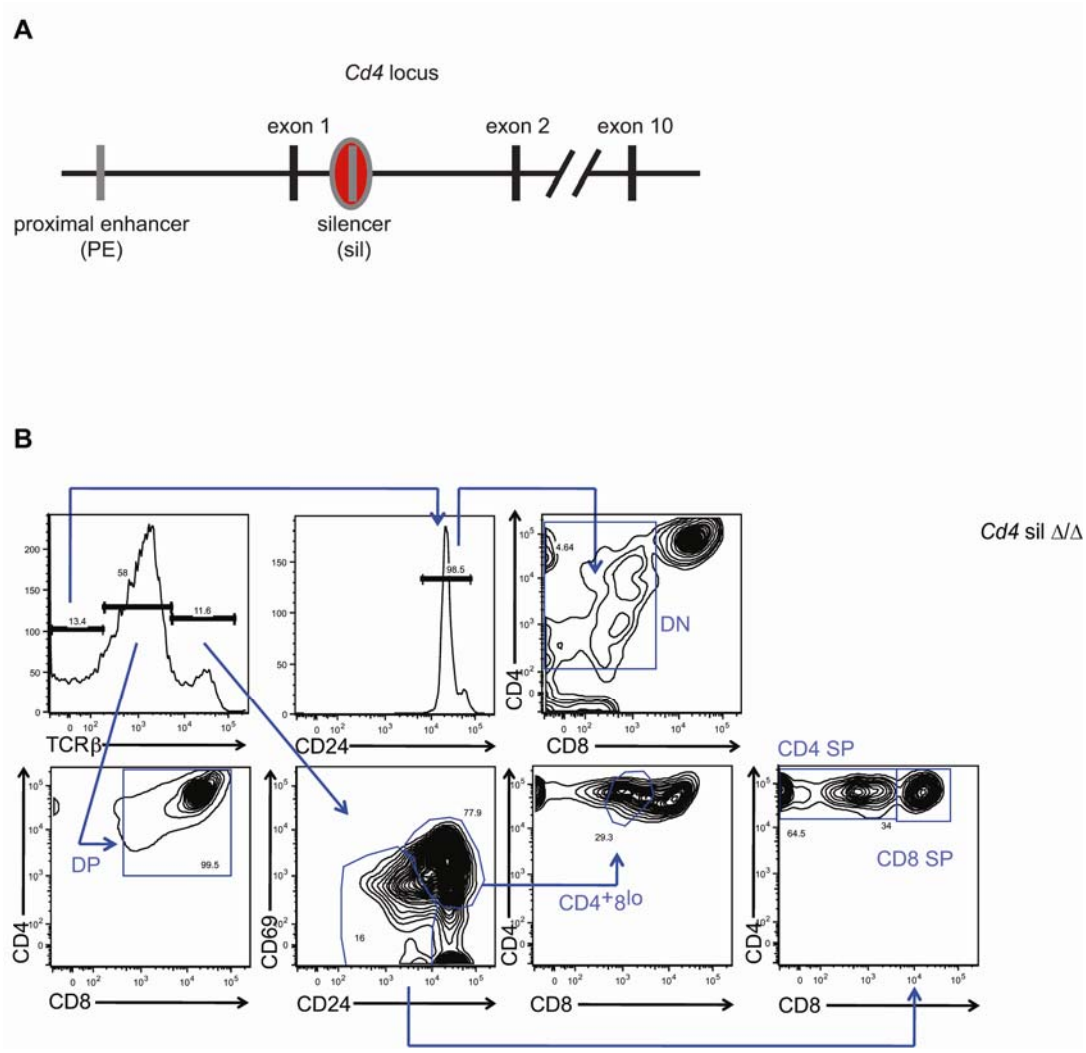

Figure S6. Scheme of the *Cd4* locus showing the silencer (sil) and sorting strategy for *Cd4* PE deficient thymocytes, related to Figure 6

(A) Scheme of the *Cd4* locus showing the position of the silencer (PE) deleted in *Cd4* sil Δ/Δ.

(B) For *Cd4* sil deficient cells, DN were sorted as TCRb^{lo}CD24^{+}CD8$^{–}$, DP as TCRb^{int}CD4^{+}CD8^{+}, CD4^{+}8^{lo} as TCRb^{hi}CD24^{+}CD69^{+}CD4^{+}8^{lo}, CD4 SP as TCRb^{hi}CD24$^{–}$CD69$^{–}$CD4^{+}CD8$^{–}$, and CD8 SP as TCRb^{hi}CD24$^{–}$CD69$^{–}$CD8^{+}.

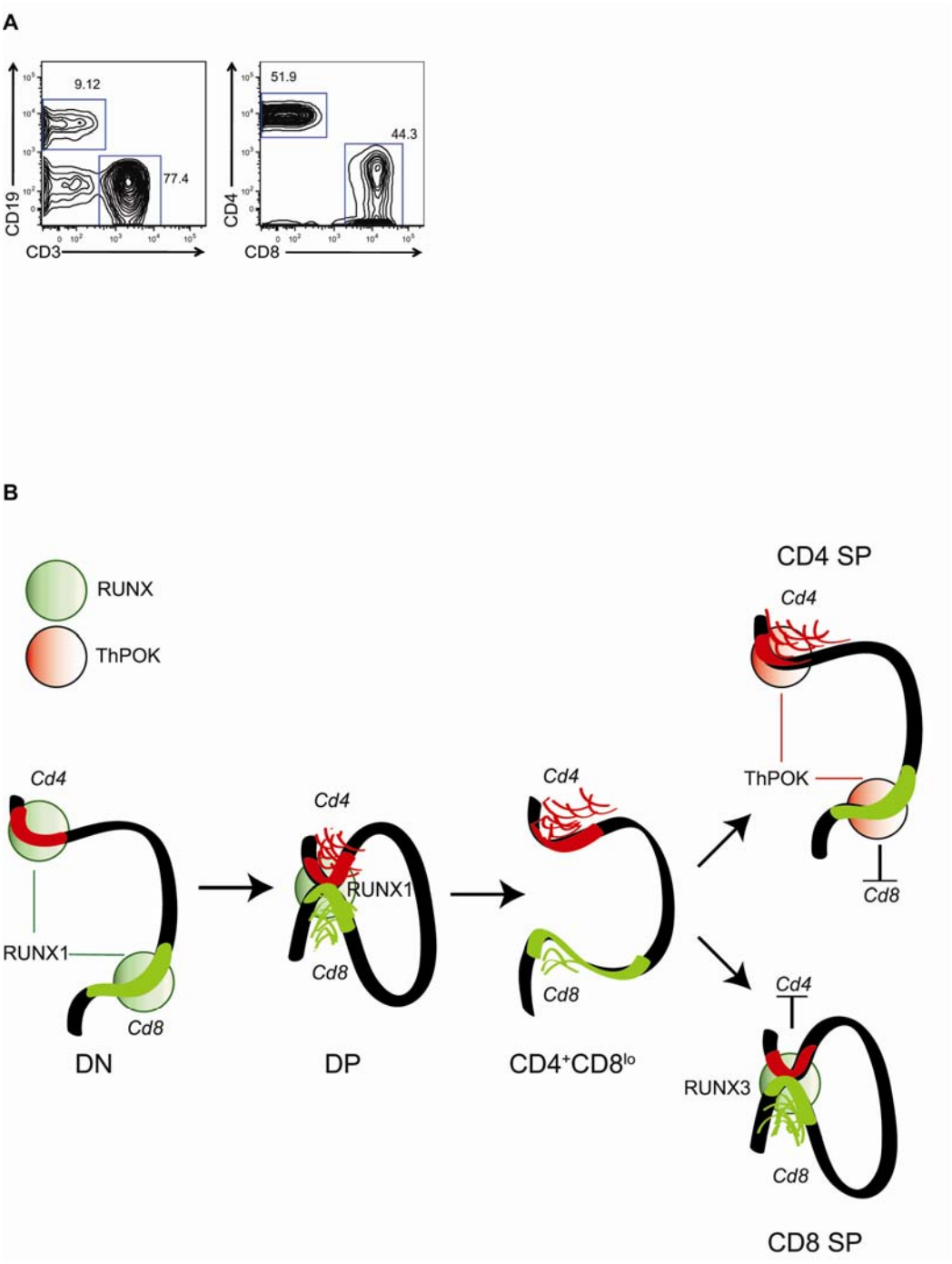

Figure S7. Sorting strategy for human lymphocytes CD8$^+$ T cells, CD4$^+$ T cells, or B cells and a model of *Cd4-Cd8* association during T cell development, related to Figure 7

(A) On a live lymphocyte gate, human B cells were sorted as CD3$^-$CD19$^+$, and T cells were sorted as either CD19$^-$ CD3$^+$CD4$^+$CD45RA$^+$CD54RO$^-$ for CD4$^+$ cells or CD19$^-$CD3$^+$CD8$^+$CD45RA$^+$CD54RO$^-$ for CD8$^+$ cells.

(B) Model of *Cd4-Cd8* association during T cell development.

Table S1. *Cd4* or *Cd8* recruitment to pericentromeric heterochromatin in wild-type murine thymocytes, including percentages and statistical analyses, related to Figure 1

A. Recruitment of *Cd4* to pericentromeric heterochromatin in WT cells

Cell type	No recruitment		Monoallelic		Biallelic		Sample size (cells)
	number	(%)	number	(%)	number	(%)	
DN	40	(51)	31	(39)	8	(10)	79
DP	114	(73)	41	(26)	2	(1)	157
$CD4^+CD8^{lo}$	75	(64)	36	(31)	6	(5)	117
CD4 SP	83	(64)	42	(32)	5	(4)	130
CD8 SP	39	(36)	63	(59)	5	(5)	107

B. Statistical analysis of *Cd4* recruitment to pericentromeric heterochromatin in WT cells

Cell type 1		Cell type 2	*P* value
DN	versus	DP	9.79e-04
		$CD4^+CD8^{lo}$	2.21e-01
		CD4 SP	1.41e-01
		CD8 SP	4.61e-02
DP	versus	$CD4^+CD8^{lo}$	2.05e-01
		CD4 SP	2.96e-01
		CD8 SP	1.20e-07
$CD4^+CD8^{lo}$	versus	CD4 SP	9.78e-01
		CD8 SP	1.79e-04
CD4 SP	versus	CD8 SP	2.25e-04

C. Recruitment of *Cd8* to pericentromeric heterochromatin in WT cells

Cell type	No recruitment		Monoallelic		Biallelic		Sample size (cells)
	number	(%)	number	(%)	number	(%)	
DN	59	(72)	20	(24)	3	(4)	82
DP	94	(61)	55	(36)	5	(3)	154
$CD4^+CD8^{lo}$	39	(30)	75	(58)	16	(12)	130
CD4 SP	45	(36)	71	(57)	9	(7)	125
CD8 SP	64	(61)	34	(32)	7	(7)	105

D. Statistical analysis of *Cd8* recruitment to pericentromeric heterochromatin in WT cells

Cell type 1		Cell type 2	*P* value
DN	versus	DP	2.62e-01
		$CD4^+CD8^{lo}$	6.00e-08
		CD4 SP	7.19e-06
		CD8 SP	4.14e-01
DP	versus	$CD4^+CD8^{lo}$	1.09e-06
		CD4 SP	3.43e-04
		CD8 SP	5.93e-01
$CD4^+CD8^{lo}$	versus	CD4 SP	4.19e-01
		CD8 SP	2.98e-05
CD4 SP	versus	CD8 SP	9.50e-04

E. Statistical analysis of *Cd4* versus *Cd8* recruitment to pericentromeric heterochromatin in WT cells

Cell type	*P* value
DN	3.69e-02
DP	1.34e-01
$CD4^+CD8^{lo}$	1.42e-06
CD4 SP	1.15e-04
CD8 SP	1.05e-03

Table S2. *Cd4* or *Cd8* recruitment to pericentromeric heterochromatin in wild-type, $E8_I$ deficient, and $E8_IE8_{II}$ double mutant thymocytes, including percentages and statistical analyses, related to Figure 2

A. Recruitment of *Cd4* to pericentromeric heterochromatin in DP cells

Genotype	No recruitment		Monoallelic		Biallelic		Sample size (cells)
	number	(%)	number	(%)	number	(%)	
WT	95	(66)	43	(30)	6	(4)	144
$CD8^+$ $E8_I$ Δ/Δ $E8_{II}$ Δ/Δ	85	(65)	41	(31)	5	(4)	131
$CD8^{lo}$ $E8_I$ Δ/Δ $E8_{II}$ Δ/Δ	107	(67)	47	(29)	6	(4)	160

B. Statistical analysis of *Cd4* recruitment to pericentromeric heterochromatin in DP cells

Genotype 1		Genotype 2	*P* value
WT	versus	$CD8^+$ $E8_I$ Δ/Δ $E8_{II}$ Δ/Δ	9.82e-01
WT	versus	$CD8^{lo}$ $E8_I$ Δ/Δ $E8_{II}$ Δ/Δ	9.94e-01
$CD8^+$ $E8_I$ Δ/Δ $E8_{II}$ Δ/Δ	versus	$CD8^{lo}$ $E8_I$ Δ/Δ $E8_{II}$ Δ/Δ	9.38e-01

C. Recruitment of *Cd8* to pericentromeric heterochromatin in DP cells

Genotype	No recruitment		Monoallelic		Biallelic		Sample size (cells)
	number	(%)	number	(%)	number	(%)	
WT	108	(65)	51	(31)	7	(4)	166
$CD8^+$ $E8_I$ Δ/Δ $E8_{II}$ Δ/Δ	57	(48)	55	(47)	6	(5)	118
$CD8^{lo}$ $E8_I$ Δ/Δ $E8_{II}$ Δ/Δ	55	(35)	91	(57)	13	(8)	159

D. Statistical analysis of *Cd8* recruitment to pericentromeric heterochromatin in DP cells

Genotype 1		Genotype 2	*P* value
WT	versus	$CD8^+$ $E8_I$ Δ/Δ $E8_{II}$ Δ/Δ	2.60e-02
WT	versus	$CD8^{lo}$ $E8_I$ Δ/Δ $E8_{II}$ Δ/Δ	6.90e-07
$CD8^+$ $E8_I$ Δ/Δ $E8_{II}$ Δ/Δ	versus	$CD8^{lo}$ $E8_I$ Δ/Δ $E8_{II}$ Δ/Δ	9.91e-02

Table S3. *Cd4* recruitment to pericentromeric heterochromatin in wild-type, *Zbtb7b*$^{hd/hd}$ and ThPOK transgenic thymocytes, including percentages and statistical analyses, related to Figure 4

A. Recruitment of *Cd4* to pericentromeric heterochromatin in CD4 SP cells

Genotype	No recruitment		Monoallelic		Biallelic		Sample size (cells)
	number	(%)	number	(%)	number	(%)	
WT	96	(60)	59	(37)	5	(3)	160
Zbtb7b$^{hd/hd}$	40	(31)	76	(59)	12	(9)	128

B. Statistical analysis of *Cd4* recruitment to pericentromeric heterochromatin in CD4 SP cells

Genotype 1		Genotype 2	*P* value
WT	versus	*Zbtb7b*$^{hd/hd}$	1.14e-05

Table S4. *Cd4* recruitment to pericentromeric heterochromatin in wild-type and *Cd4* PE deficient thymocytes, including percentages and statistical analyses, related to Figure 5

A. Recruitment of *Cd4* to pericentromeric heterochromatin

Cell type	Genotype	No recruitment		Monoallelic		Biallelic		Sample size (cells)
		number	(%)	number	(%)	number	(%)	
DN	WT	82	(51)	56	(35)	23	(14)	161
	Cd4 PE Δ/Δ	45	(39)	55	(48)	14	(12)	114
DP	WT	81	(64)	41	(33)	4	(3)	126
	Cd4 PE Δ/Δ	73	(63)	39	(34)	4	(3)	116
$CD4^{+}CD8^{lo}$	WT	86	(64)	43	(32)	6	(4)	135
	Cd4 PE Δ/Δ	36	(41)	40	(46)	11	(13)	87
CD4 SP	WT	78	(61)	46	(36)	4	(3)	128
	Cd4 PE Δ/Δ	47	(42)	54	(48)	11	(10)	112
CD8 SP	WT	56	(43)	59	(46)	14	(11)	129
	Cd4 PE Δ/Δ	56	(38)	76	(51)	16	(11)	148

B. Statistical analysis of *Cd4* recruitment to pericentromeric heterochromatin

Genotype 1	Cell type 1		Genotype 2	Cell type 2	*P* value
WT	DN	versus	*Cd4* PE Δ/Δ	DN	7.83e-02
	DP	versus		DP	9.70e-01
	$CD4^{+}CD8^{lo}$	versus		$CD4^{+}CD8^{lo}$	5.26e-03
	CD4 SP	versus		CD4 SP	1.15e-02
	CD8 SP	versus		CD8 SP	6.14e-01

Table S5. *Cd8* recruitment to pericentromeric heterochromatin in wild-type and *Cd4* sil deficient thymocytes, including percentages and statistical analyses, related to Figure 6

A. Recruitment of *Cd8* to pericentromeric heterochromatin

Cell type	Genotype	No recruitment		Monoallelic		Biallelic		Sample size (cells)
		number	(%)	number	(%)	number	(%)	
DN	WT	52	(50)	47	(45)	6	(6)	105
	Cd4 sil Δ/Δ	66	(50)	55	(42)	10	(8)	131
DP	WT	71	(68)	32	(30)	2	(2)	105
	Cd4 sil Δ/Δ	90	(49)	76	(41)	18	(10)	184
$CD4^{+}CD8^{lo}$	WT	56	(42)	63	(48)	13	(10)	132
	Cd4 si Δ/Δ	41	(33)	66	(53)	17	(14)	124
CD4 SP	WT	43	(37)	61	(53)	12	(10)	116
	Cd4 si Δ/Δ	46	(30)	80	(52)	27	(18)	153
CD8 SP	WT	88	(55)	65	(41)	6	(4)	159
	Cd4 sil Δ/Δ	64	(40)	76	(47)	21	(13)	161

B. Statistical analysis of *Cd8* recruitment to pericentromeric heterochromatin

Genotype 1	Cell type 1		Genotype 2	Cell type 2	*P* value
WT	DN	versus	*Cd4* sil Δ/Δ	DN	9.29e-01
	DP	versus		DP	5.00e-03
	$CD4^{+}CD8^{lo}$	versus		$CD4^{+}CD8^{lo}$	2.63e-01
	CD4 SP	versus		CD4 SP	1.82e-01
	CD8 SP	versus		CD8 SP	3.26e-03